

Electronic Supporting Information

for

Pomelo peels-derived, N-doped biochar microspheres as efficient and durable metal-free ORR catalysts in microbial fuel cells

Yuyuan Zhang^{a,b}, Lifang Deng^{b,*}, Huawen Hu^{a,*}, Yu Qiao^c, Haoran Yuan^b, Dongchu Chen^a, Menglei Chang^a, Hongyang Wei^a

^a School of Materials Science and Energy Engineering, Foshan University, Foshan, Guangdong 528000, China

^b CAS Key Laboratory of Renewable Energy, Guangzhou Institute of Energy Conversion, Guangzhou, Guangdong 510640, China

^c State Key Laboratory of Coal Combustion, Huazhong University of Science and Technology, Wuhan, Hubei 430074, China

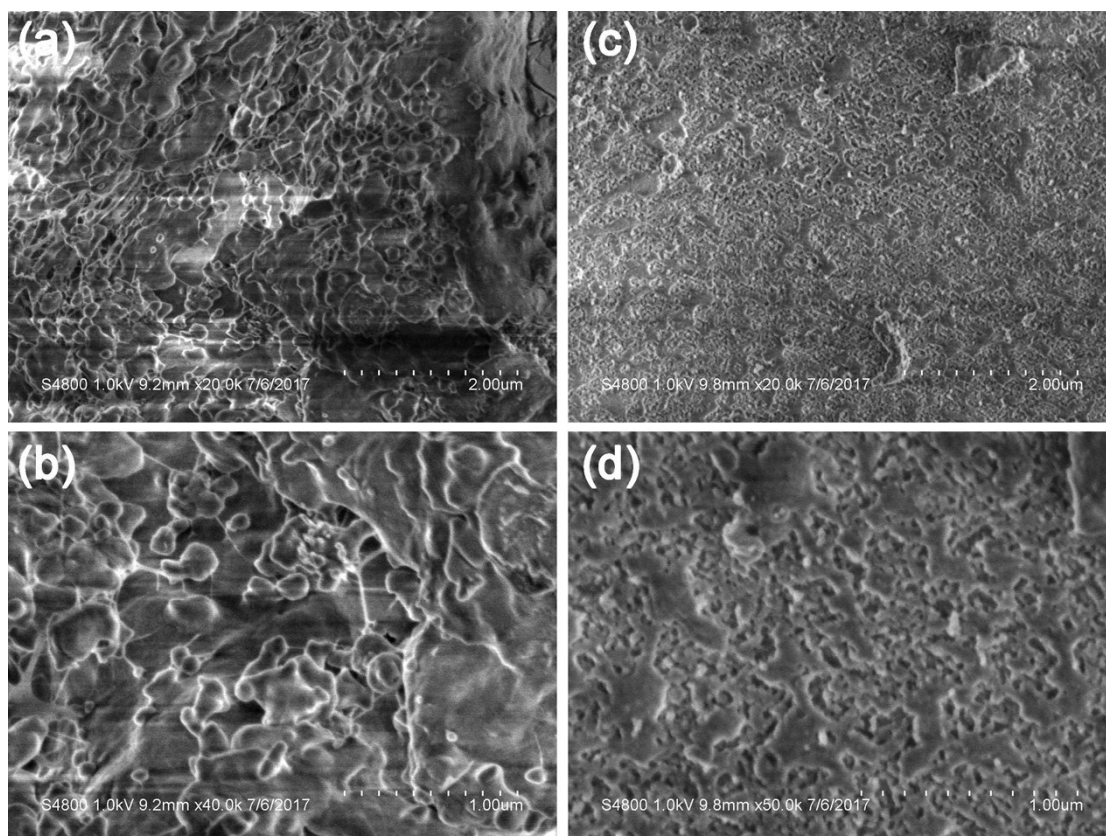


Figure S1. SEM images of the hydrothermal products starting from two different types of biomasses as control, namely durian shell (a,b) and coconut shell (c,d). The hydrothermal processing of all of these control samples could not lead to the generation of carbon-rich microspheric structure, in clear contrast to the well-formed carbon-based microspheres using pomelo peel as the starting biomass.

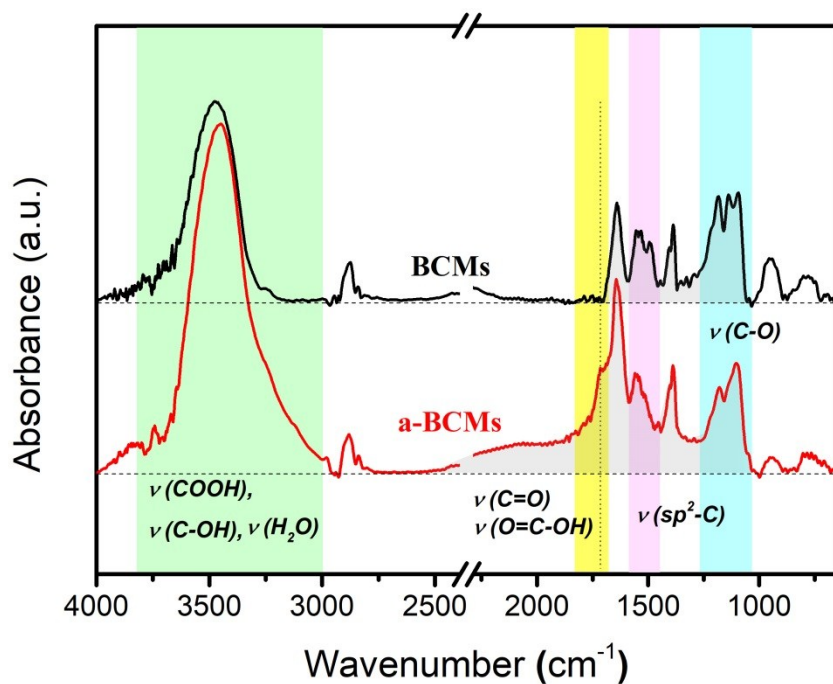


Figure S2. FTIR spectra of the BCMs and a-BCMs samples. The attribution of the absorption bands are also indicated, where $\nu(sp^2-C)$ represents stretching vibration from sp^2 -conjugated carbon domains, corresponding to the FTIR absorption band around 1550 cm^{-1} (highlighted with yellow shading).

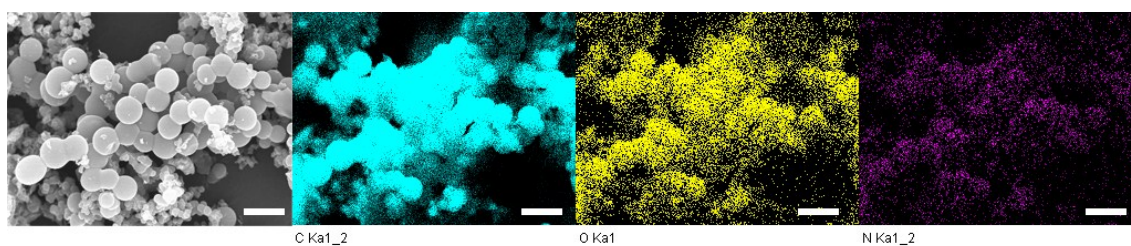


Figure S3. EDX elemental mapping images of a-BCMs; the scale bar in all the images is $5\text{ }\mu\text{m}$.

Table S1. Summary of the performances of the MFCs equipped with the control cathodic catalyst Pt/C, and with the pomelo peels-derived cathodic catalysts BCMs and a-BCMs.

Cathodic catalysts	CV (V vs. Ag/AgCl)	LSV (V vs. Ag/AgCl)	n	P_{\max} (mW·m ⁻²)
Pt/C	-0.12	-0.03	3.72	1022.9
BCMs	-0.37	-0.23	2.90	596.6
a-BCMs	-0.28	-0.08	3.52	907.2

Note: n represents electron transfer number and P_{\max} designates the maximum power density.

Table S2. Comparison of the a-BCMs-based cathode performance with those from the literature.

Cathode Catalyst	Cathode area (cm ²)	MFC reactor Volume (mL)	P_{max}	$P/P_{Pt/C}^f$ (%)	Ref.
WRC400 ^{a)}			182 mW/m ³	/	<i>Applied Energy</i> , 2019, 242, 516-525
WRC500 ^{b)}			195mW/m ³	/	
WRC600 ^{c)}	25	350	192 mW/m ³	/	
WRC700 ^{d)}			262 mW/m ³	/	
Pt/C			/	/	
PAC-800 ^{e)}	/	28	800 mW/m ²	73	<i>RSC Adv.</i> , 2017,7, 13383-13389
Pt/C			1100 mW/m ²		
(NH ₄) ₃ PO ₄ -carbon			2293±50 mW/m ²	136	<i>J. Power Source</i> , 2015, 273, 1189-1193
NH ₄ Cl-carbon			801±13 mW/m ²	48	
H ₃ PO ₄ -carbon	/	/	872±15 mW/m ²	52	
Free-carbon			715±18 mW/m ²	43	
Pt/C			1680±32 mW/m ²		
TMC900 ^{f)}			703 ± 16 mW/m ²	107	<i>Applied Catalysis B: Environmental</i> , 2016, 181, 635-643
AMC900 ^{g)}	7	28	494 ± 32 mW/m ²	75	
Pt/C			656 ± 24 mW/m ²		
BCMs			596.6 mW/m ²	58	This study
a-BCMs	7	28	907.2 mW/m ²	89	
Pt/C			1022.9 mW/m ²		

Note:

- a) Watermelon rind-derived carbon with thermal treatment at 400 °C;
b) Watermelon rind-derived carbon with thermal treatment at 500 °C;
c) Watermelon rind-derived carbon with thermal treatment at 600 °C;
d) Watermelon rind-derived carbon with thermal treatment at 700 °C;
e) Nitrogen-doped porous activated carbon derived from cocoon silk;
f) Moss-derived biocarbon material prepared by a combined hydrothermal and 900 °C thermal process;
g) Moss-derived biocarbon material prepared by a direct thermal annealing process at 900 °C;
h) The ratio of the maximum power density with the biochar-based cathode to that with the Pt/C cathode, which is proportional to the biochar-based cathode performance.

References:

1. Q. Liu, Y. Zhou, S. Chen, Z. Wang, H. Hou and F. Zhao, *J. Power Sources*, 2015, 273, 1189-1193.
2. P. Fu, L. Zhou, L. Sun, B. Huang and Y. Yuan, *RSC Adv.*, 2017, 7, 13383-13389.
3. L. Zhou, P. Fu, D. Wen, Y. Yuan and S. Zhou, *Appl. Catal. B*, 2016, 181, 635-643.
4. K. Zhong, M. Li, Y. Yang, H. Zhang, B. Zhang, J. Tang, J. Yan, M. Su and Z. Yang, *Appl. Energ.*, 2019, 242, 516-525.